# Short-period disturbances trapped in the edge region of stratospheric polar vortices

Yoshihiro Tomikawa* and Kaoru Sato†

## Abstract

A global distribution and seasonal variability of short-period ($<$ 2 days) disturbances in the lower and middle stratosphere are investigated using 6-hourly European Centre for Medium-Range Weather Forecasts reanalysis data over 15 years (1979–1993). Two-dimensional spectral analysis and recently-developed Lagrangian-mean diagnostic are used for the analysis. It is shown that the short-period disturbances are most active around the polar-night jet in each winter hemisphere. They have a wave-like structure in the zonal direction with typical zonal wavelengths of about 2,000 km (i.e., zonal wavenumber 10) and a meridionally evanescent structure with a half width of about 1,500 km, suggesting that they are waves trapped in the edge region of the polar vortex where the meridional gradient of isentropic potential vorticity is maximized. The trapped waves have a nearly barotropic structure over a depth greater than 10 km.

## 1 Introduction

Medium-scale waves dominant around the midlatitude tropopause at about 10 km height have been reported during the last decade [*Sato et al.*, 1993, 2000]. They have almost neutral structure with typical zonal wavelengths of 2,000–3,000 km and ground-based wave periods of 20–30 h, and exist in both hemispheres throughout the year. *Sato et al.* [1998, 2000] indicated that the medium-scale waves are most active around the tropopause at slightly higher latitudes than the midlatitude jet where the meridional gradient of quasi-geostrophic potential vorticity is maximized. This fact suggests that the medium-scale waves are waves trapped around the midlatitude tropopause. Because the polar vortex has large meridional gradients of isentropic potential vorticity (PV) in its edge region, it is naturally expected that similar small-scale trapped waves exist there.

In this study, we investigate the characteristics of short-period ($<$ 2 days) disturbances observed around the polar-night jet and show that they are trapped in the large meridional gradients of PV there.

*Research Center of Advanced Science and Technology, University of Tokyo, Tokyo, Japan (e-mail: tomikawa@nipr.ac.jp)

†National Institute of Polar Research, Tokyo, Japan (e-mail: kaoru@nipr.ac.jp)

## 2 Data

Used are the ECMWF reanalysis basic level III data (initialized analysis upper air data) with a time interval of 6 h (0000, 0600, 1200, and 1800 UTC). The data are distributed on a $2.5^\circ \times 2.5^\circ$ latitude and longitude mesh at 17 pressure levels (1000, 925, 850, 775, 700, 600, 500, 400, 300, 250, 200, 150, 100, 70, 50, 30, and 10 hPa). The dataset covers 15 years from 1 January 1979 through 31 December 1993. The reanalysis data, whose quality can be expected to be uniform for a long term, are suitable to examine the climatology of dynamical characteristics of atmospheric phenomena in terms of global distribution and seasonal variation.

## 3 Spectral analysis

Figure 1 shows a zonal wavenumber-frequency power spectrum of isentropic relative vorticity at $60^\circ$S at $\theta$ = 540 K ($z$ = 21–22 km, where $z$ is the altitude) in austral winter (June, July, and August) averaged over 15 years (1979–1993). The latitude of $60^\circ$S nearly corresponds to the polar vortex edge in the southern hemisphere as shown later. An isentropic relative vorticity is used to examine disturbances throughout this paper. PV may be more appropriate for the analysis than relative vorticity, because PV is closely related to the wave activity and its propagation characteristics [cf., *Andrews et al.*, 1987]. However, because PV is a nonlinear quantity defined as a product of isentropic absolute vorticity by static stability, noise in the ECMWF data is emphasized especially in small-scale structures. A prominent peak is observed in the region with long positive wavelength ($>$ 2,000 km) and long period ($>$ 2 days) corresponding to eastward-propagating planetary-scale and synoptic-scale disturbances. Another continuous peak, that has phase velocities of about 40 m s$^{-1}$, is observed in the region with short positive wavelength ($\approx$ 2,000 km) and short period ($<$ 1 day) corresponding to eastward-propagating small-scale disturbances. The spectral density is large also in the region with short negative wavelength ($>$ -2,000 km) and short period ($<$ 2 days). This feature is considered to be aliasing of eastward-propagating ultra-short-period ($<$ 0.5 day) disturbances into westward-propagating short-period ($<$ 2 days) ones, because the spectral peak of eastward-propagating disturbances connects smoothly with that of westward-propagating ones across the Nyquist frequency ($=$ 2 day$^{-1}$).

In this study, the eastward-propagating disturbances with

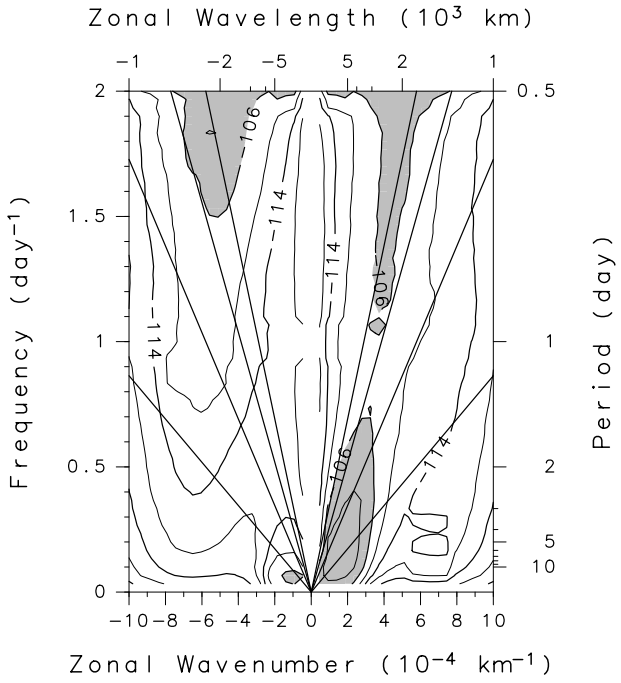


Figure 1: Two-dimensional power spectrum of isentropic relative vorticity in the energy-content form as a function of zonal wavenumber ($10^{-4}$ km$^{-1}$) and frequency (day$^{-1}$) at $60°$S at $\theta$ = 540 K in austral winter (June, July, and August) averaged over 15 years (1979–1993). Positive and negative wavenumbers represent the eastward and westward propagations, respectively. Top and right axes represent the zonal wavelength and ground-based wave period, respectively. Contour intervals are 4 dB. Regions with values larger than -106 dB are shaded. Thick solid lines show ground-based phase velocities of $\pm$10, $\pm$20, $\pm$30, and $\pm$40 m s$^{-1}$.

short periods ($<$ 2 days) and short wavelengths ($\approx$ 2,000 km) are analyzed in detail. To extract the short-period disturbances, a high-pass filter with a cutoff period of 48 h was applied to the time series instead of a spatial filter in the zonal direction. This is because the isolation of spectral peaks of large- and small-scale disturbances is more obvious in frequency than in wavenumber and because the filtering in the zonal direction is not appropriate when the deformation of polar vortex is large. Note that this time filter also extracts eastward-propagating ultra-short-period ($<$ 0.5 day) disturbances aliased into the negative zonal wavenumber region of the spectrum without losing their amplitudes. In the stratosphere, thermal tides are observed at periods of 24 h and 12 h. Thus, prior to extracting short-period ($<$ 2 days) disturbances, we removed the tidal components whose phases are fixed to local time, by applying a high-pass filter with a cutoff period of 10 days to each time series (0000, 0600, 1200, and 1800 UTC) separately. Hereafter, we refer to the disturbances with periods shorter than 2 days in which the tidal components are not included, simply as “short-period disturbances”.

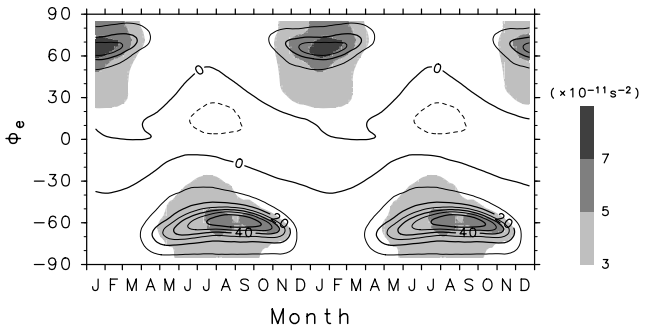


Figure 2: Time-equivalent latitude section of tangential wind (contours) and Lagrangian-mean squared fluctuations of isentropic relative vorticity (shades) on the 540 K isentropic surface averaged over 15 years (1979–1993). Two cycles of the year are drawn. Contour intervals are 10 m s$^{-1}$.

# 4 Lagrangian-mean description

## 4.1 Time-equivalent latitude section

Figure 2 shows a time-equivalent latitude ($\phi_e$) section of tangential wind and Lagrangian-mean squared fluctuations of isentropic relative vorticity at $\theta$ = 540 K averaged over 15 years (1979–1993). A tangential wind is defined as a mean horizontal wind tangent to each equivalent latitude contour on a given isentropic surface. The tangential winds in northern and southern hemispheres have maximum speeds of 30–40 m s$^{-1}$ around $\phi_e$ = 65°N in January and February and of 60–70 m s$^{-1}$ around $\phi_e$ = 60°S in August and September, respectively. Time periods when a strong tangential wind is observed are longer in the southern hemisphere (8 months from April through November) than in the northern hemisphere (5 months from November through March). We refer to those periods as a polar vortex season. The peaks of tangential wind in both hemispheres moved slightly equatorward and poleward during the first and last halves of the polar vortex season, respectively. These interhemispheric differences in the characteristics of tangential wind imply that the polar vortex in the southern hemisphere is more stable and isolated from middle latitudes than that in the northern hemisphere.

The relative vorticity fluctuation has maximum intensity almost at the same time and at the same equivalent latitude as the tangential wind in both hemispheres. Contrary to the tangential wind, however, the peak amplitudes of relative vorticity fluctuations are larger in the northern hemisphere than in the southern hemisphere. Another interesting feature is that the latitudes where relative vorticity fluctuations have large amplitudes extend to equatorward of 30° latitude in both hemispheres.

## 4.2 Equivalent latitude-potential temperature section

Figure 3 shows equivalent latitude ($\phi_e$)-potential temperature ($\theta$) sections of tangential wind and Lagrangian-mean squared fluctuations of isentropic relative vorticity in Jan-

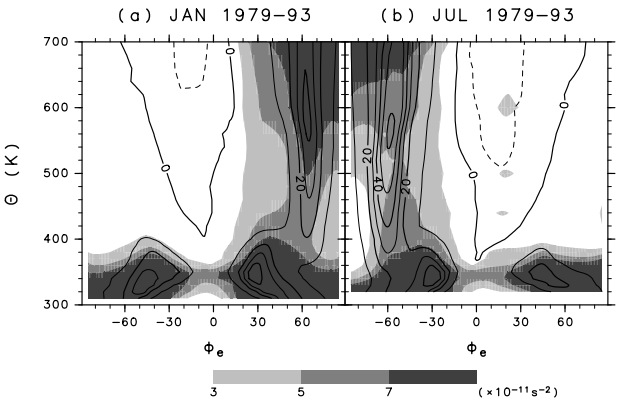


Figure 3: Equivalent latitude-potential temperature sections of tangential wind (contours) and Lagrangian-mean squared fluctuations of isentropic relative vorticity (shades) in (a) January and (b) July averaged over 15 years (1979–1993). Contour intervals are 10 m $s^{-1}$.

uary and July averaged over 15 years (1979–1993). The tangential wind speed has a maximum in the height region of $\theta > 400$ K in each winter hemisphere, corresponding to the polar-night jet. The peak of relative vorticity fluctuations due to the short-period disturbances is observed where the tangential wind is maximized in both winter hemispheres. The equatorward extension of large amplitudes of relative vorticity fluctuations is also seen on all isentropic surfaces above 400 K in both winter hemispheres. The amplitudes of relative vorticity fluctuations increase with potential temperature above 400 K. Another peak of tangential wind associated with the subtropical jet is located at $\theta \approx 340$ K in middle latitude region of both hemispheres. Around the subtropical jet, a notable peak of relative vorticity fluctuations is observed, which is likely due to the medium-scale waves reported first by *Sato et al.* [1993] as mentioned in section 1.

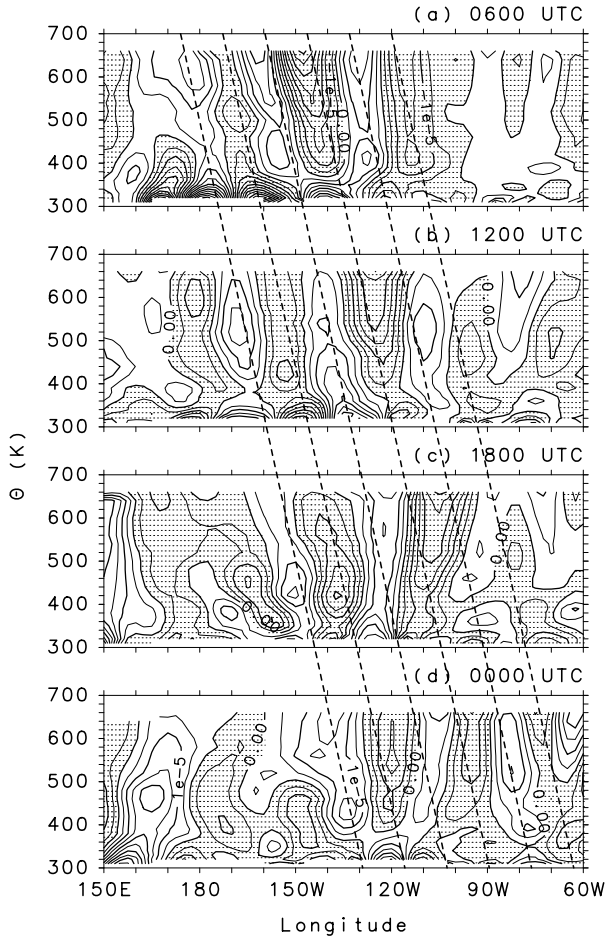


Figure 4: Longitude-potential temperature sections of isentropic relative vorticity fluctuations along 60°S at (a) 0600 UTC, (b) 1200 UTC, (c) 1800 UTC on 18 July 1993, and (d) 0000 UTC on 19 July 1993. Contour intervals are $5 \times 10^{-6}$ $s^{-1}$. Negative regions are shaded. Dashed lines show the eastward propagation of positive and negative peaks.

# 5 Structure of short-period disturbances

## 5.1 Typical example of short-period disturbance

Figure 4 shows a series of the longitude-potential temperature ($\theta$) section of relative vorticity fluctuations from 0600 UTC on 18 to 0000 UTC on 19 July 1993 in the longitude region of 150°E-60°W at 60°S. The relative vorticity disturbances propagate eastward, and have a zonal wavelength of about 1,500 km (longitudinal width of about 27 degrees at 60°S). It seems that the phase tilt of the disturbances is small throughout this period (i.e., nearly barotropic) although the disturbances at higher isentropic surfaces propagate eastward slightly faster than those at lower isentropic surfaces. The ground-based phase velocity around the 540 K isentropic surface is about 62 degrees per day, that is, about 40 m $s^{-1}$. Their bottom and top are around $\theta$ = 400 K (15–16 km) and higher than $\theta$ = 700 K (27–28 km), respectively. Such nearly barotropic disturbances can often be seen around the polar vortex edge.

## 5.2 Composite analysis

To examine the mean feature of three-dimensional structure of short-period disturbances, we make composite maps of relative vorticity fluctuations in the longitude-potential temperature, latitude-potential temperature, and longitude-latitude sections. The grid points having a significant maximum of relative vorticity fluctuation component ($> 5 \times 10^{-6}$ $s^{-1}$) in the region of 90°W-180°W and 50°S-70°S at $\theta$ = 540 K, where the clear wave-like structure was observed in Fig. 4, are chosen as a reference point for the composite. Figure 5 is the result made from 91 figures in July 1993. Solid lines show the relative vorticity fluctuations. Dashed lines in Figs. 5b and 5c show the composite zonal wind and potential vorticity, respectively. The reference point is marked with "+". Note that the choice of

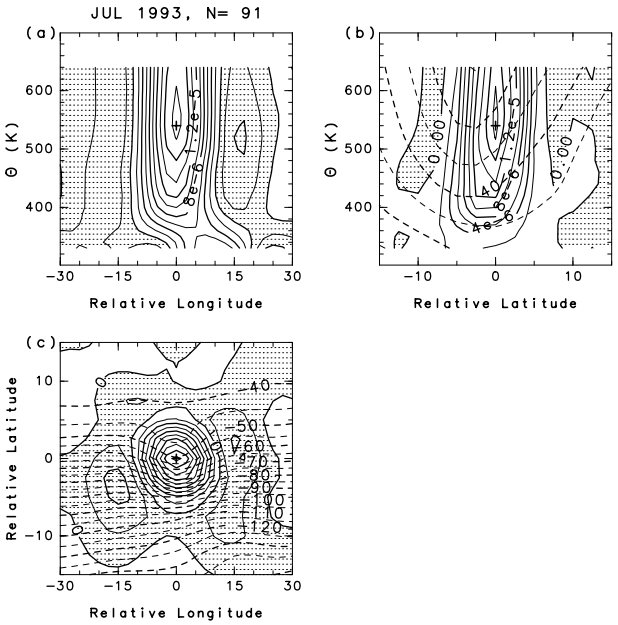


Figure 5: Composite (a) longitude-potential temperature, (b) latitude-potential temperature, and (c) longitude-latitude sections of isentropic relative vorticity fluctuations (solid line) in July 1993 mapped onto the relative positions to the reference point marked by "+", where the isentropic relative vorticity fluctuation is maximized in the region of 90°W-180°W and 50°S-70°S on the 540 K isentropic surface and more than $5 \times 10^{-6}$ s$^{-1}$. Dashed lines show (b) the zonal wind and (c) background potential vorticity. Contour intervals are $2 \times 10^{-6}$ s$^{-1}$ for isentropic relative vorticity fluctuations, 10 m s$^{-1}$ for zonal wind, and 5 PVU (1 PVU = $10^{-6}$ K kg$^{-1}$ m$^2$s$^{-1}$) for potential vorticity. N is the number of projected figures.

month, longitude range, and threshold value for the reference point has little influence on the composite structure.

From the longitude-potential temperature section (Fig. 5a), it is obvious that the relative vorticity fluctuations have a wave-like structure and little phase tilt in the zonal direction. The zonal wavelength is about 2,000 km (longitudinal width of 35 degrees). Amplitudes of negative peaks on both sides of the reference point are reduced compared with the positive peak because of superposition of disturbances with slightly different zonal wavelengths.

In the latitude-potential temperature section (Fig. 5b), the relative vorticity fluctuations have an evanescent structure and little phase tilt in the meridional direction. The meridional half width is about 1,500 km (latitudinal width of 14 degrees). The peak of background zonal wind shown by dashed lines is nearly lying on the reference latitude (= 0°). The relative vorticity fluctuations are extended down to the region lower than $\theta$ = 400 K (15–16 km) and up to the region higher than $\theta$ = 700 K (27–28 km), respectively.

Figure 5c shows composite of the horizontal structure of relative vorticity fluctuations (solid lines) and background PV (dashed lines). The background PV gradients are maximized around the reference point where the relative vorticity fluctuations are also maximized. The relative vorticity fluctuations have little meridional phase tilt. This means that the short-period disturbances are nearly barotropic and suggests that there are little meridional momentum and heat fluxes associated with the short-period disturbances. Similar three-dimensional structure is observed throughout the polar vortex season (not shown).

# 6 Concluding remarks

The short-period ($<$ 2 days) disturbances dominant around the polar-night jet were investigated using 6-hourly ECMWF reanalysis data covering 15 years (1979–1993). The short-period disturbances are most active around the polar-night jet where the meridional PV gradients are maximized. The short-period disturbances have a zonally wave-like structure with typical wavelengths of about 2,000 km (i.e., zonal wavenumber 10) and a meridionally evanescent structure with a half width of about 1,500 km around the polar-night jet. These features indicate that the short-period disturbances are waves meridionally trapped around the polar-night jet.

The source and sink of the short-period disturbances will be discussed in detail in the presentation.

## Acknowledgments

The data used in this study were provided by ECMWF. GFD-DENNOU Library was used for drawing figures. This research was supported by Grant-in-Aid for Scientific Research (B)(2) 12440126 of the Ministry of Education, Culture, Sports, Science and Technology, Japan.

# References

[1] Andrews, D. G., J. R. Holton, and C. B. Leovy, *Middle Atmosphere Dynamics*, 489 pp., Academic, San Diego, Calif., 1987.

[2] Sato, K., H. Eito, and I. Hirota, Medium-Scale Travelling Waves in the Extra-Tropical Upper Troposphere, *J. Meteor. Soc. Japan, 71*, 427–436, 1993.

[3] Sato, K., H. Yazawa, and T. Matsuno, Trapping of the medium-scale waves into the tropopause, *Abstracts, Rossby-100 Symp.*, Vol. II, Stockholm, Sweden, Stockholm University, 302–304, 1998.

[4] Sato, K., K. Yamada, and I. Hirota, Global Characteristics of Medium-Scale Tropopausal Waves Observed in ECMWF Operational Data, *Mon. Weather Rev., 128*, 3808–3823, 2000.